

The Impact of Lime Content in Cement Mortar on the Shear Stress and Ductility of Perforated Brick Masonry Wallets

Maissene Benhadji

Built Environment Research Laboratory (LBE), Civil Engineering Faculty, USTHB, Algeria
maissene.benhadji@gmail.com

Omar Bouksani

Department of Civil Engineering, Faculty of Technology, Yahia Fares University, Medea Algeria, Built Environment Research Laboratory (LBE), Civil Engineering Faculty, USTHB
omarbouksani14@gmail.com (corresponding author)

Fattoum Kharchi

Built Environment Research Laboratory (LBE), Civil Engineering Faculty, USTHB, Algeria
kharchifcong@yahoo.fr

Farid Belhamel

National Center of Studies and Integrated Research on Building Engineering, Algeria
belhameldz@yahoo.fr

Received: 16 May 2025 | Revised: 10 June 2025 | Accepted: 15 June 2025

Licensed under a CC-BY 4.0 license | Copyright (c) by the authors | DOI: <https://doi.org/10.48084/etasr.11024>

ABSTRACT

The partial replacement of cement with lime can offer significant advantages in restoring historic masonry, as traditional mortar compositions were predominantly lime-based. This study examines how incorporating lime into jointing mortar affects the shear behavior of masonry wallets subjected to diagonal tensile tests. To this end, masonry wallets were constructed using mortars in which lime replaced cement at levels of 0%, 10%, 20%, 30%, and 40% by weight. The mechanical properties of the mortars were assessed through compressive and flexural strength tests and the shear behavior of the wallets was evaluated using diagonal tensile tests. The results indicate that substituting cement with lime increases the mortar ductility. Furthermore, the diagonal tensile tests showed that integrating lime into the mortars improves the overall performance of the masonry, suggesting that lime could be used as an alternative to restore historic masonry structures.

Keywords-masonry; mortar; lime; brick; diagonal tensile test; shear stress; ductility

I. INTRODUCTION

Masonry is a traditional construction technique commonly found in historical buildings, which is still used in urban and rural structures. Like all buildings, masonry structures are under the pressure of various loads, such as winds, seismic activity, and soil sliding. Authors in [1, 2] examined the seismic damage, such as diagonal cracking, joint sliding, and brick crushing, in masonry structures as a result of weak bonds or inadequate materials, underlying the importance of post-earthquake damage assessments to understand their structural behavior and develop effective repair strategies. Authors in [3-5] investigated this behavior through experimental shear strength tests, including triplet shear tests and diagonal tensile

tests [6, 7], which provided data and deformation characteristics of the masonry walls. Authors in [8-11] showed that the shear behavior of the brick masonry depends on the bricks, the mortar, and the quality of their bond, which relies on the physical and mechanical properties of the brick units and mortar, as well as the cohesion and friction within the masonry. Using non-standard bricks [12], such as full clay bricks [13], calcium silicate bricks [14, 15], ceramic bricks [16], self-insulating concrete units [17], pumice bricks [18], and regular and irregular stone units [19], reduces the shear strength of the masonry. Conversely, authors in [20-22] stated that low-strength mortar has an insignificant impact on the mechanical properties of the masonry, while authors in [23, 24] indicated that low-strength mortar can reduce the shear strength.

However, it has been demonstrated that low-strength mortar may enhance the ductility of the masonry compared to high-strength mortar [25]. Authors in [26, 27] found that, while high-strength mortar increases the shear stress in the masonry, it reduces ductility, resulting in a more brittle behavior. Preserving a historic masonry and building new structures that imitate traditional techniques requires the utilization of compatible bricks and mortar to ensure long-term structural integrity. Due to the limited research on the effect of the lime content in the mortar on the ultimate drift and displacement ductility of perforated brick masonry walls, this study aims to advance heritage conservation by partially replacing cement with lime. Masonry wall specimens were subjected to diagonal tensile testing in accordance with ASTM E 519-02 [28]. This research assesses the influence of varying lime content on the shear strength, ultimate drift, and displacement ductility.

II. EXPERIMENTAL DETAILS

A. Material Properties

In this study, perforated clay bricks measuring 210 mm×105 mm×55 mm were used, and the mortar binder was composed of a blend of cement and lime. The lime used was of the aerial variety, classified as CL70 according to the EN 459-1 standard [29], with a density of 750 kg/m³. Regarding cement, it was a CEM II A/42.5, with a bulk density of 1450 kg/m³. The chemical compositions of lime and cement are presented in Table I. Furthermore, the sand utilized in this study was of a crushed calcareous nature, with a maximum nominal particle size of 5 mm.

TABLE I. CHEMICAL COMPOSITIONS OF LIME AND CEMENT

Oxide element	Lime (%)	Cement (%)
CaO	73.3	59.7
MgO	0.5	1.11
Fe ₂ O ₃	2	3.81
SiO ₂	2.5	18.57
Al ₂ O ₃	1.5	4.28
SO ₃	0.5	2.43
Na ₂ O	0.4	0.22
K ₂ O	--	0.9
CO ₂	5	--

B. Mortar Preparation

The experiment included five mortar mixes with varying percentages of aerial lime (CL70). Lime was used as a partial replacement for cement, with substitution levels ranging from 0% to 40% by weight. For each mix formulation, three specimens were prepared and tested to ensure the repeatability and reduce the variability in the results. The detailed compositions of the different mortar mixes are presented in Table II.

In order to simulate the typical conditions that are encountered in the manufacturing of masonry mortar, they/the mixtures were prepared manually in two successive homogenization steps. Initially, the sand and aerial lime were thoroughly amalgamated, then cement was added and the dry mixture was remixed to ensure homogeneity. Subsequently, water was added gradually, with the mixture being tested until

its workability was comparable to that of the control mortar. The flow time measured using the LCPC workability meter ranged from 12 s to 13 s. Subsequent to the completion of the mixing sequences, the fresh mortar mixtures were cast into 40×40×160 mm prismatic molds, which were sealed with humid jute sheets for a period of 24 h. The specimens were subjected to a curing regimen within a controlled laboratory setting at a temperature of 20°C and a relative humidity of 65% until the testing phase.

TABLE II. MORTAR MIXTURE PROPORTIONS

Mortar designation	Materials (g)			
	Cement	Lime	Sand	Water
M-L0	450	0	1350	225
M-L10	405	45	1350	238
M-L20	360	90	1350	241
M-L30	315	135	1350	249
M-L40	271	179	1350	258

C. Testing Method of Mortars

The mechanical properties of mortars with varying lime content were determined at the ages of 7, 14, 28, and 90 days after demolding. The flexural and compressive strength tests were conducted in accordance with the EN 1015-11 standard [30]. Flexural strength tests were conducted on mortar prisms with dimensions of 40 mm×40 mm×160 mm. Subsequently, the compressive strength of the half-prisms obtained after splitting during the flexural test was measured.

D. Shear Strength Test on Wallets

To examine the masonry behavior under shear loads, a diagonal tensile test was conducted on square wallet specimens. Initially, rectangular wallet specimens with dimensions of 29 cm by 42 cm were constructed with 1-cm-thick mortar joints. To ensure the preservation of the joint integrity, the specimens were left for a period of 90 days. Subsequently, the wallet specimens were cut into square specimens measuring 29 cm by 29 cm using a marble saw equipped with a diamond blade, as shown in Figure 1. The shear strength of the samples was evaluated using a diagonal tensile test, in accordance with the ASTM E 519-02 standard [28]. The wallet undergoes a 45° rotation, and the diagonal tensile load is attributed to a compressive load applied through a 50-ton hydraulic jack along one of its diagonals. The test setup entailed the usage of two steel loading shoes, strategically positioned at the top and bottom corners of the rotated wallet. Additionally, two dial gauges were used to assess the shortening and elongation of the wallet under shear loading, as depicted in Figure 2. To determine the mechanical properties of the masonry, the shear stress-shear strain curves were plotted. The shear strength (τ) and shear strain (γ_{sh}), shear modulus (G), and ductility (μ_u) were defined as:

- The shear strength (τ) is calculated from the diagonal load (P) and the net area of the wallets (A_n):

$$\tau = \frac{0.707 \times P}{A_n} \quad (1)$$

where the net area (A_n) is calculated as:

$$A_n = \frac{w+h}{2} \times t \times n \quad (2)$$

where w , h , and t represent the width, height, and thickness of the square wallets, respectively. Also, n represents the percent of the gross area of the unit that is solid.

- The shear strain or angular strain (γ_{sh}) is assessed from the horizontal elongation (ΔH), the vertical shortening (ΔV), and the gauge length (g):

$$\gamma_{sh} = \varepsilon_x + \varepsilon_y = \frac{\Delta H}{g_x} + \frac{\Delta V}{g_y} = \frac{\Delta H + \Delta V}{g} \quad (3)$$

- The shear modulus (G), also known as modulus of rigidity, is defined as the slope of the shear stress-shear strain curve in the elastic phase. It is calculated using a secant line intersecting the curve at 10% of the maximum shear stress:

$$G = \frac{\tau}{\gamma_{sh}} \quad (4)$$

- The Young's modulus (E) can be related to the shear modulus by:

$$E = 2G(1 + \nu) \quad (5)$$

- The displacement ductility ratio (μ_u) is defined as the ratio of the ultimate diagonal displacement (ΔV_u) and the displacement at yield (ΔV_y) as:

$$\mu_u = \frac{\Delta V_u}{\Delta V_y} \quad (6)$$

- The ultimate drift γ_u is defined at peak shear stress and is calculated by dividing the ultimate diagonal displacement by the height of the wallet specimens:

$$\gamma_u = \frac{\Delta u}{H} \quad (7)$$

where Δu represents the diagonal displacement corresponding to the ultimate strength, and H is the height of the wallet.

III. RESULTS AND DISCUSSION

A. Mechanical Properties of Brick Units

In accordance with the EN 772-1 standard [31], the perforated bricks were subjected to compressive and flexural strength tests. The values of the compressive strength, flexural strength, and modulus of elasticity of the brick units were measured and are illustrated in Table III.

TABLE III. PHYSICAL AND MECHANICAL CHARACTERISTICS OF BRICK UNITS

Characteristics	Values
Density (kg/m ³)	1820
Compressive strength (MPa)	16.8
Flexural strength (MPa)	4
Elasticity modulus (GPa)	14.2

B. Compressive Strength of Mortars

Figure 3 presents the failure mode of the mortar under compressive testing, while Figure 4 portrays the compressive strength at 7, 14, 28, and 90 days of curing for mortars

containing 0%, 10%, 20%, 30%, and 40% lime as a partial cement replacement. It has been observed that increasing the lime content results in a reduction in compressive strength. For instance, at 28 days, the compressive strength of mortars with 10%, 20%, 30%, and 40% lime decreased by 10%, 23%, 37%, and 56%, respectively, compared to the cement mortar with 0% lime.

However, this decrease in compressive strength has a negligible effect on the overall bearing capacity of the masonry. Authors in [32] found that the compressive strength of the mortar contributes only a negligible amount to the overall compressive strength of the masonry assemblies. Furthermore, the mechanical behavior of the masonry is primarily influenced by the compressive strength of the bricks themselves rather than that of the mortar [33, 34]. Consequently, the mortar serves as a binding agent, while the bricks are the primary contributors to the masonry's strength.

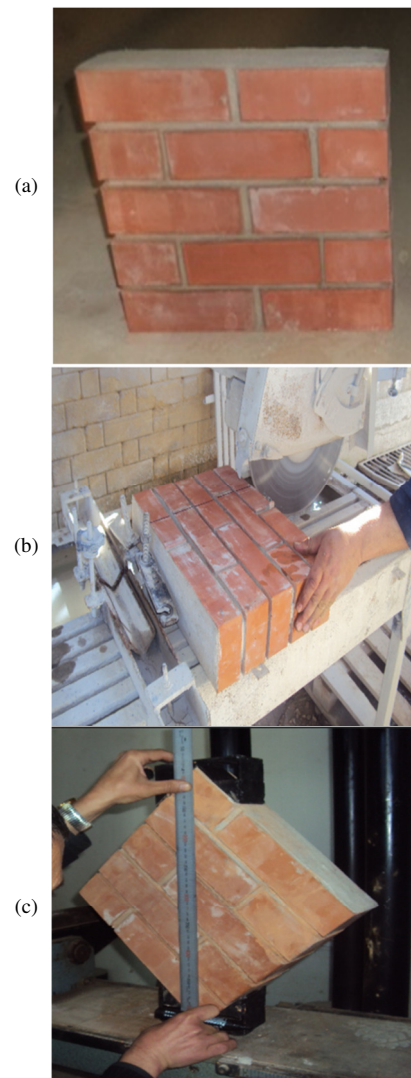


Fig. 1. Wallet masonry specimen: (a) initial manufactured wallet 290mm x 420 mm, (b) cutting with marble saw, and (c) square specimen 290 cm x 290cm.

C. Flexural Strength of Mortars

As depicted in Figure 5, the failure mode of the mortar under flexural testing is evident. Figure 6 presents the flexural strength outcomes at 7, 14, 28, and 90 days of curing for mortars that incorporate 0%, 10%, 20%, 30%, and 40% lime as a partial replacement for cement.

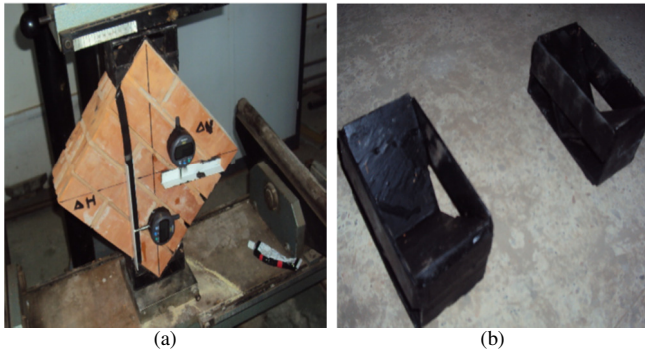


Fig. 2. Diagonal tensile test devices: (a) horizontal and vertical gauges, and (b) metallic shoes.

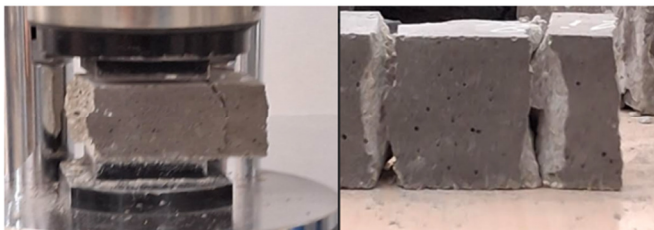


Fig. 3. Failure mode of mortar in compressive test.

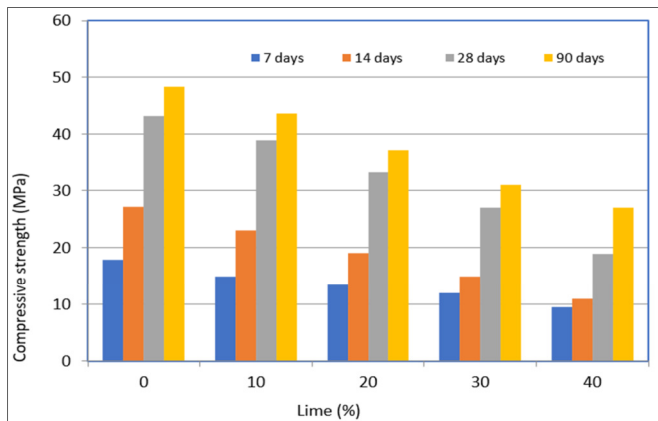


Fig. 4. Compressive strength for mortars with different percentages of lime at: 7, 14, 28, and 90 days.

The flexural strength of all cement-lime mortars was found to be significantly lower than that of the pure cement mortar. At the 28-day mark, the flexural strength of mortars containing 10%, 20%, 30%, and 40% lime exhibited a decline of 16%, 31%, 45%, and 55%, respectively, in comparison to the cement mortar composed of 0% lime.

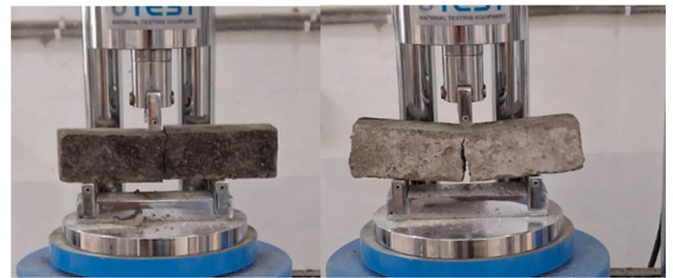


Fig. 5. Failure mode of mortar in flexural test.

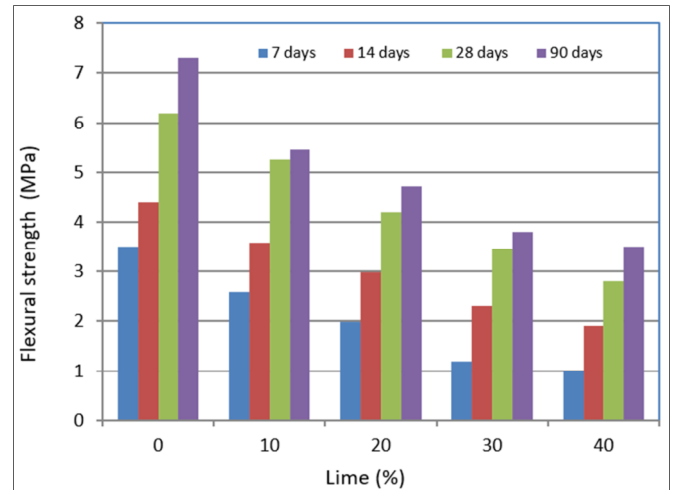


Fig. 6. Flexural strength for mortars with different percentages of lime at: 7, 14, 28, and 90 days.

D. Stiffness and Ductility of Mortars

Although the peak compressive and flexural strengths have been shown to decrease, Figure 7 demonstrates that increasing the lime content enhances the ductility of the mortars. First, regarding the initial slope of the mortar curves with and without lime, the reduction in Young's modulus indicates a decrease in the mortar stiffness. Furthermore, the post-peak behavior of the mortars with varying lime content exhibited a more gradual softening compared to the cement mortar (0% lime), which exhibited brittle failure characterized by a sudden drop in stress. The hypothesis that the addition of lime to the cement mortar enhances its ductility and flexibility is supported by empirical evidence. Furthermore, the compressive tests demonstrated that the ultimate strain increased from 2.8% for the mortars with 0% lime to 6.2% for those containing 40% lime. In flexural strength tests, the ultimate strain exhibited an increase from 0.13 to 0.4%.

E. Diagonal Tensile of Brick Masonry Wallets

Figures 8 and 9 show the experimental shear stress-shear strain curves and failure modes of the wallet specimens subjected to diagonal tensile tests, respectively.

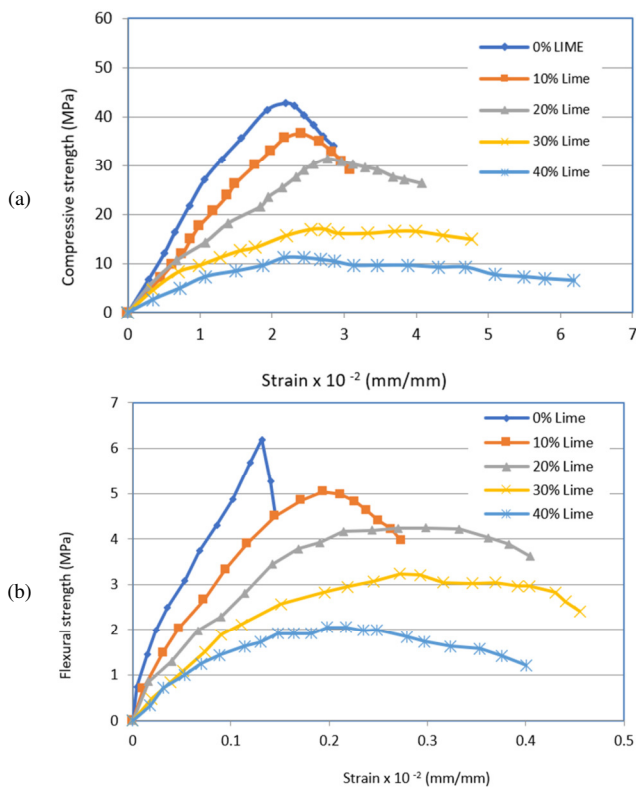


Fig. 7. Stress-strain curves at 28 days for mortars with different lime content: (a) compressive, (b) flexural.

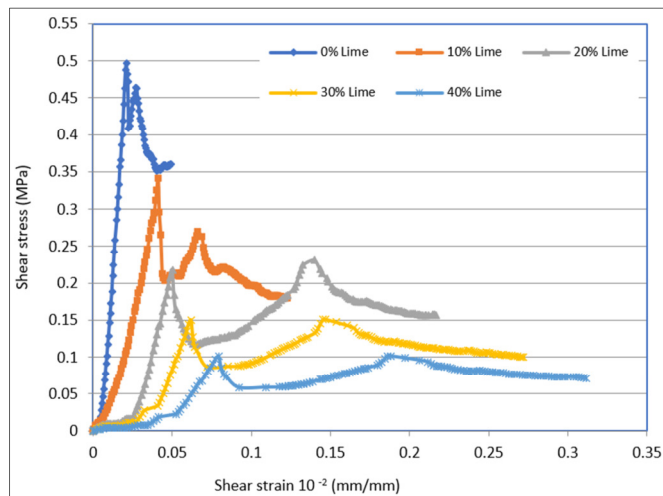


Fig. 8. Stress-strain curves for wallets bonded with mortar and varying lime content.

The wallet specimens bonded with cement-based mortar (0% lime) exhibited a nearly linear shear stress–strain relationship up to a peak shear stress of 0.497 MPa, followed by a rebound peak and then a sudden stress drop, indicating brittle behavior. This response is likely attributable to the inherent fragility of the mortar lacking lime. Conversely, the specimens bonded with mortar containing lime exhibited reduced peak shear stresses. Specifically, the peak shear stress values decreased by 31%, 59%, 69%, and 79%, respectively,

for the wallets bonded with mortar containing lime contents of 10%, 20%, 30%, and 40%. This decline in peak stress is likely attributable to the reduced mechanical strength of the mortars containing lime. However, an increase in the lime content in mortars has been observed to enhance the post-peak behavior of the masonry, resulting in a more ductile response that can be proved advantageous in seismic contexts. The failure mode appears to initiate with the deterioration of the horizontal joints, subsequently progressing to the involvement of the vertical joints. The failure of the horizontal mortar joint corresponds to the first peak in the experimental shear stress–shear strain curve, while the failure of the vertical joint can be related to the second peak. Furthermore, the observed ductility can be attributed to the use of mortar containing lime, as well as to the interlocking of cracked surfaces along the vertical joints.

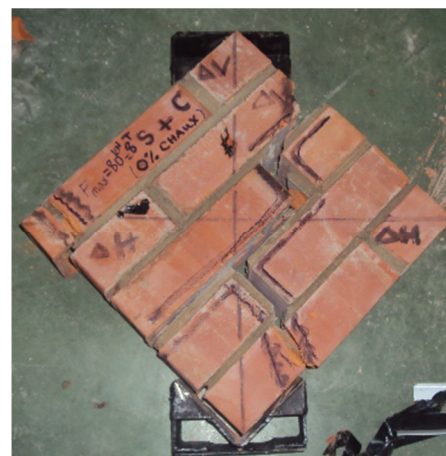


Fig. 9. Shear sliding failure in horizontal and vertical joint mortar for masonry wallets.

F. Shear Modulus of Brick Masonry Wallet

However, despite the reduction in peak shear stress, the addition of lime to the mortar enhanced the flexibility of the wallets. Figures 10-12 present the shear modulus, drift at peak shear stress, and displacement ductility ratio, respectively. These figures indicate that the wallets bonded with mortars containing different lime contents showed an increase in their flexibility. The shear modulus exhibited a decline as the lime content in the mortar increased. Specifically, the shear modulus of the wallets bonded with cement mortar was 5.2 GPa, but decreased to 4.9 GPa, 4.2 GPa, and 2.5 GPa for wallets bonded with mortar containing 20, 30, and 40% lime, respectively.

G. Drift at Peak Shear Stress of Masonry Wallets

Masonry wallets bonded with mortars containing lime demonstrated higher drift at peak shear stress compared to those bonded with cement mortar, which exhibited a drift of 0.15%. Specifically, the drift values observed for the masonry with mortar containing 10%, 20%, 30%, and 40% lime were 0.21%, 0.35%, 0.57%, and 0.72%, respectively.

H. Displacement Ductility Ratio of Brick Masonry Wallet

The presence of lime in mortars results in wallet failure at larger displacements, which indicates an increase in ductility.

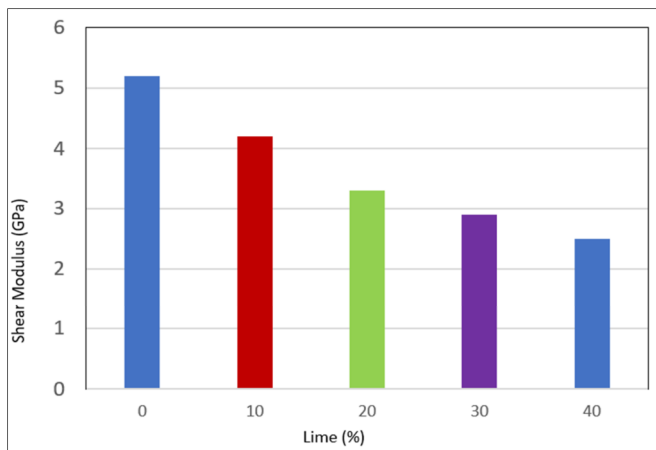


Fig. 10. Shear modulus for wallets bonded with mortar and varying lime content.

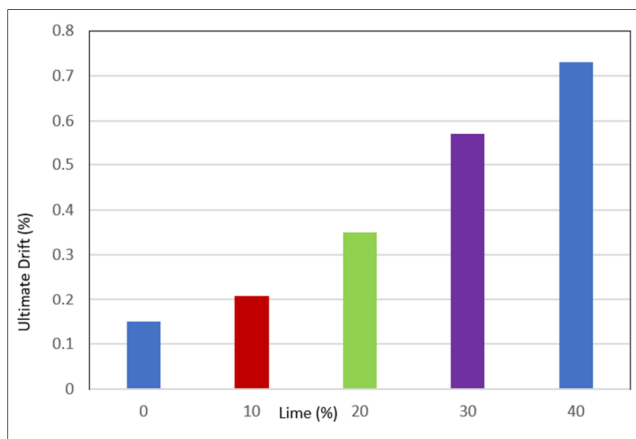


Fig. 11. Ultimate drift at peak shear stress for wallets bonded with mortar and varying lime content.

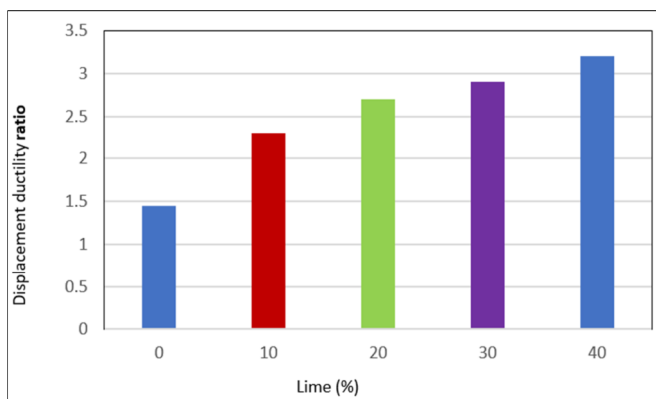


Fig. 12. Displacement ductility ratio for wallets bonded with mortar and varying lime content.

The wallet specimens bonded with lime-containing mortars exhibited a gradual loss of shear strength in comparison to those bonded with cement mortar, which experienced a sudden drop in the shear stress and brittle failure. In accordance to previous findings, a displacement ductility ratio of 1.45 was

observed for masonry wallets bonded with cement mortar. In contrast, wallets with cement replaced by 10%, 20%, 30%, and 40% lime exhibited increased displacement ductility ratio values of 2.3, 2.7, 2.9, and 3.2, respectively.

IV. CONCLUSIONS

Based on the experimental results, the following conclusions were drawn:

- The mortars containing lime as a partial replacement for cement exhibited reduced compressive and flexural strengths in comparison with cement-based mortars. This decrease was significant as the lime content increased.
- The mortars with lime exhibited a tendency toward more ductile failure modes when subjected to compressive and flexural tests, suggesting a partial replacement of cement content with lime.
- The analysis revealed that the specimens bonded with lime-containing mortars exhibited greater drift at peak shear stress compared to those bonded with cement-based mortars. This observation suggests an improvement in the flexibility of the masonry, possibly attributable to the presence of lime in mortar joints.
- The specimens with mortar containing lime exhibited an increase in the displacement ductility ratio with an increase in the lime content. Although this suggests a potentially beneficial effect of lime on ductility, further testing is necessary to verify this observation statistically.

REFERENCES

- [1] B. Atmaca *et al.*, "Field Observations and Numerical Investigations on Seismic Damage Assessment of RC and Masonry Minarets During the February 6th, 2023, Kahramanmaraş (Mw 7.7 Pazarcık and Mw 7.6 Elbistan) Earthquakes in Türkiye," *International Journal of Architectural Heritage*, vol. 19, no. 7, pp. 1117–1142, Jul. 2025, <https://doi.org/10.1080/15583058.2024.2337651>.
- [2] V. Kahya *et al.*, "Evaluation of earthquake-related damages on masonry structures due to the 6 February 2023 Kahramanmaraş-Türkiye earthquakes: A case study for Hatay Governorship Building," *Engineering Failure Analysis*, vol. 156, Feb. 2024, Art. no. 107855, <https://doi.org/10.1016/j.engfailanal.2023.107855>.
- [3] L. Pelà, K. Kasioumi, and P. Roca, "Experimental evaluation of the shear strength of aerial lime mortar brickwork by standard tests on triplets and non-standard tests on core samples," *Engineering Structures*, vol. 136, pp. 441–453, Apr. 2017, <https://doi.org/10.1016/j.engstruct.2017.01.028>.
- [4] D. V. Bompa and A. Y. Elghazouli, "Experimental and numerical assessment of the shear behaviour of lime mortar clay brick masonry triplets," *Construction and Building Materials*, vol. 262, Nov. 2020, Art. no. 120571, <https://doi.org/10.1016/j.conbuildmat.2020.120571>.
- [5] G. Andreotti, F. Graziotti, and G. Magenes, "Detailed micro-modelling of the direct shear tests of brick masonry specimens: The role of dilatancy," *Engineering Structures*, vol. 168, pp. 929–949, Aug. 2018, <https://doi.org/10.1016/j.engstruct.2018.05.019>.
- [6] G. Lee, J. H. Park, K. V. A. Pham, C. H. Lee, and K. Lee, "Experimental Investigation of Traditional Clay Brick and Lime Mortar Intended for Restoration of Cultural Heritage Sites," *Applied Sciences*, vol. 11, no. 13, Jan. 2021, Art. no. 6228, <https://doi.org/10.3390/app11136228>.
- [7] R. D. Pasquantonio, G. A. Parsekian, F. S. Fonseca, and N. G. Shrive, "Experimental and numerical characterization of the interface between concrete masonry block and mortar," *Revista IBRACON de Estruturas e Materiais*, vol. 13, pp. 578–592, Jul. 2020, <https://doi.org/10.1590/S1983-41952020000300008>.

- [8] J. Diaz-Basteris, B. Menéndez, J. Reyes, and J. C. Sacramento Rivero, "A Selection Method for Restoration Mortars Using Sustainability and Compatibility Criteria," *Geosciences*, vol. 12, no. 10, Oct. 2022, Art. no. 362, <https://doi.org/10.3390/geosciences12100362>.
- [9] P. B. Lourenço, "Computational Strategies for Masonry Structures," Ph.D. dissertation, Delft University of Technology, Netherlands, 1996.
- [10] R. Amiraslanzadeh, E. Rin, T. Ikemoto, and M. Miyajima, "Experimental and numerical analysis of mechanical interaction of masonry bricks and mortar," in *10th International Symposium on Mitigation of Geo-disasters in Asia*, Kyoto, Japan, Oct. 2012.
- [11] F. Saviano, G. P. Lignola, and F. Parisi, "Experimental compressive and shear behaviour of clay brick masonry with degraded joints," *Construction and Building Materials*, vol. 452, Nov. 2024, Art. no. 138880, <https://doi.org/10.1016/j.conbuildmat.2024.138880>.
- [12] T. M. Shah, A. Kumar, S. N. R. Shah, A. A. Jhatial, and M. H. Janwery, "Evaluation of the Mechanical Behavior of Local Brick Masonry in Pakistan," *Engineering, Technology & Applied Science Research*, vol. 9, no. 3, pp. 4298–4300, Jun. 2019, <https://doi.org/10.48084/etasr.2850>.
- [13] R. Capozucca, "Shear Behaviour of Historic Masonry Made of Clay Bricks," *Open Construction & Building Technology Journal*, vol. 5, no. 1, pp. 89–96, Oct. 2011, <https://doi.org/10.2174/1874836801105010089>.
- [14] A. H. Salmanpour, N. Mojsilović, and J. Schwartz, "Displacement capacity of contemporary unreinforced masonry walls: An experimental study," *Engineering Structures*, vol. 89, pp. 1–16, Apr. 2015, <https://doi.org/10.1016/j.engstruct.2015.01.052>.
- [15] V. Zijl and G. P. A. G., "Modeling Masonry Shear-Compression: Role of Dilatancy Highlighted," *Journal of Engineering Mechanics*, vol. 130, no. 11, pp. 1289–1296, Nov. 2004, [https://doi.org/10.1061/\(ASCE\)0733-9399\(2004\)130:11\(1289\)](https://doi.org/10.1061/(ASCE)0733-9399(2004)130:11(1289)).
- [16] M. Shabdin, M. Zargarán, and N. K. A. Attari, "Experimental diagonal tension (shear) test of Un-Reinforced Masonry (URM) walls strengthened with textile reinforced mortar (TRM)," *Construction and Building Materials*, vol. 164, pp. 704–715, Mar. 2018, <https://doi.org/10.1016/j.conbuildmat.2017.12.234>.
- [17] A.-B. Abdelmoneim Elamin Mohamad and Z. Chen, "Experimental and Numerical Analysis of the Compressive and Shear Behavior for a New Type of Self-Insulating Concrete Masonry System," *Applied Sciences*, vol. 6, no. 9, Sep. 2016, Art. no. 245, <https://doi.org/10.3390/app6090245>.
- [18] B. Demirel, "Optimization of the composite brick composed of expanded polystyrene and pumice blocks," *Construction and Building Materials*, vol. 40, pp. 306–313, Mar. 2013, <https://doi.org/10.1016/j.conbuildmat.2012.11.008>.
- [19] M. L. Beconcini, P. Croce, P. Formichi, F. Landi, and B. Puccini, "Experimental Evaluation of Shear Behavior of Stone Masonry Wall," *Materials*, vol. 14, no. 9, Jan. 2021, Art. no. 2313, <https://doi.org/10.3390/ma14092313>.
- [20] M. Ramesh, R. Ramirez, M. Azenha, and P. B. Lourenço, "Evaluating the Role of Mortar Composition on the Cyclic Behavior of Unreinforced Masonry Shear Walls," *Materials*, vol. 17, no. 18, Jan. 2024, Art. no. 4443, <https://doi.org/10.3390/ma17184443>.
- [21] M. Ramesh, M. Parente, M. Azenha, and P. B. Lourenço, "Influence of Lime on Strength of Structural Unreinforced Masonry: Toward Improved Sustainability in Masonry Mortars," *Sustainability*, vol. 15, no. 21, Jan. 2023, Art. no. 15320, <https://doi.org/10.3390/su152115320>.
- [22] A. Zagaroli, J. Kubica, I. Galman, and K. Falkjar, "Study on the Mechanical Properties of Two General-Purpose Cement–Lime Mortars Prepared Based on Air Lime," *Materials*, vol. 17, no. 5, Jan. 2024, Art. no. 1001, <https://doi.org/10.3390/ma17051001>.
- [23] L. Lavado and J. Gallardo, "Shear strength of brick mortar interface for masonry in Lima city," *TECNIA*, vol. 29, no. 2, pp. 59–64, Aug. 2019, <https://doi.org/10.21754/tecnia.v29i2.707>.
- [24] V. Alecci, M. Fagone, T. Rotunno, and M. De Stefano, "Shear strength of brick masonry walls assembled with different types of mortar," *Construction and Building Materials*, vol. 40, pp. 1038–1045, Mar. 2013, <https://doi.org/10.1016/j.conbuildmat.2012.11.107>.
- [25] S. Pal, A. Yadav, and K. Saggu, "Assessment of shear bond strength of triplets using different joint thicknesses and mortar types," *Materials Research Proceedings*, vol. 49, pp. 386–395, Mar. 2025, <https://doi.org/10.21741/9781644903438-39>.
- [26] K. F. Hansen, E. Nykanen, and F. R. Gottfredsen, "Shear Behaviour of Bed Joints at Different Levels of Precompression," *Masonry International*, vol. 12, no. 2, pp. 70–78, 1998.
- [27] G. Mohamad, F. S. Fonseca, A. T. Vermeltfoort, D. R. W. Martens, and P. B. Lourenço, "Strength, behavior, and failure mode of hollow concrete masonry constructed with mortars of different strengths," *Construction and Building Materials*, vol. 134, pp. 489–496, Mar. 2017, <https://doi.org/10.1016/j.conbuildmat.2016.12.112>.
- [28] *E519/E519M-22 Standard test method for diagonal tension (Shear) in masonry assemblages*. West Conshohocken, PA, USA: ASTM International, 2022.
- [29] *BS EN 459-1:2015 Building lime - Part 1: Definitions, specifications and conformity criteria*. London, UK: BSI, 2015.
- [30] *BS EN 1015-11:2019 Methods of test for mortar for masonry - Part 11: Determination of flexural and compressive strength of hardened mortar*. London, UK: BSI, 2019.
- [31] *BS EN 772-1:2011+A1:2015 Methods of test for masonry units - Determination of compressive strength*. London, UK: BSI, 2011.
- [32] K. C. Voon, J. M. Ingham, and J. W. Butterworth, "In-plane Seismic Design of Concrete Masonry Structures," Ph.D. dissertation, University of Auckland, Auckland, New Zealand, 2007.
- [33] K. S. Gumaste, K. S. Nanjunda Rao, B. V. Venkatarama Reddy, and K. S. Jagadish, "Strength and elasticity of brick masonry prisms and wallets under compression," *Materials and Structures*, vol. 40, no. 2, pp. 241–253, Mar. 2007, <https://doi.org/10.1617/s11527-006-9141-9>.
- [34] H. B. Kaushik, D. C. Rai, and S. K. Jain, "Stress-Strain Characteristics of Clay Brick Masonry under Uniaxial Compression," *Journal of Materials in Civil Engineering*, vol. 19, no. 9, pp. 728–739, Sep. 2007, [https://doi.org/10.1061/\(ASCE\)0899-1561\(2007\)19:9\(728\)](https://doi.org/10.1061/(ASCE)0899-1561(2007)19:9(728)).